# First-principles Study of Electronic Structural and Mechanical Properties of $Mg_xLa(x=1, 2, 3)$ Compounds under Pressure

**LI Yan, ZHAO Yuhong***, YANG Xiaomin, TIAN Jinzhong

*(College of Materials Science and Engineering, North University of China, Taiyuan 030051, China)*

**Abstract:** The effects of pressure on structural, elastic and electronic properties of $Mg_xLa$ ($x$=1, 2, 3) compounds are investigated by using CASTEP program based on the density functional theory. The calculated equilibrium lattice parameters at zero pressure agree well with available experimental and theoretical values. The calculated DOS show that the structure of these compounds remains mechanically stable and structural phase transformation is not induced with increasing pressure from 0 to 30 GPa, and their structural stability increases with pressure. The ductility of MgLa can be improved by increasing pressure, which is the same as $Mg_2La$ in 0-20 GPa, while brittle behavior turns into ductile behavior in 0-5 GPa for $Mg_3La$. The resistance to volume deformation of $Mg_xLa$ ($x$=1, 2, 3) compounds can be improved as the pressure increases. The shear deformation resistance and elastic stiffness of $Mg_3La$ can be enhanced by rising pressure, but MgLa and $Mg_2La$ increase first and then decrease when pressure is up to 25 GPa. In addition, the three compounds exhibit the elastic anisotropy with pressure.

**Key words:** Mg-La alloys; elastic properties; electronic structure; first-principles

## 1 Introduction

Magnesium alloys, as the lightweight metallic structural materials, have been widely used in many fields, such as aerospace, automotive, microelectronics and communications, because they have good casting properties, high strength to weight ratio and good specific stiffness[1,2]. However, the poor strength and creep resistance at elevated temperature have limited the application of Mg-based alloys[3]. Studies have shown that adding the rare earths (RE) into magnesium alloys can significantly improve the mechanical properties at room temperature and high temperature[2,4],

and can also improve the creep resistance of Mg-based alloys[5]. Experimental investigations[6-8] found: the addition of trace amounts of the rare earth elements lanthanum(La) to Mg-based alloys can not only refine the microstructure, increase the room temperature tensile strength and yield strength but also can enhance the corrosion resistance well. Zhang *et al*[9] calculated the elastic and thermodynamic properties of $Mg_3La$ and $Mg_3Ce$ compounds. Chen *et al*[10] studied the electronic structural and mechanical properties of $Mg_2La$ and $Mg_2Sc$. S Ganeshan *et al*[11] calculated the elastic properties of MgLa, $Mg_2La$ and $Mg_3La$ phases. However, all the researches mentioned above are conducted under zero pressure. It is well known that the pressure plays an important role in affecting the material mechanical properties. So, in this paper, the first-principles calculations are investigated to study the structural, electronic and elastic properties of $Mg_xLa$ ($x$=1, 2, 3) compounds under 0-30 GPa pressure at 0 K.

## 2 Experimental

In present work, all the first-principles calculations on $Mg_xLa$ ($x$=1,2,3) are performed based on density functional theory (DFT)[12] as implemented by Cambridge Serial Total Energy Package (CASTEP)[13],

in which a plane wave ultrasoft pseudopotential[14] is used. The Perdewe-Burkee-Ernzerhof (PBE)[15] of generalized-gradient approximation (GGA)[16] is used for exchange-correlation functional. The Broyden-Fletcher-Goldfarb-Shanno (BFGS) scheme[17] is utilized to find the ground state and optimize all the crystal structure with a minimum energy, where the cutoff energy $E_{cut}$ is set to be 400 eV. The Brillouin zone sampling is performed using the Monkhorst-Pack k-point meshes, the k-point meshes for MgLa, $Mg_2La$ and $Mg_3La$ are set to be 13×13×13, 10×10×10 and 13×13×13, respectively. The self-consistent convergence of the total energy is less than $1.0×10^{-5}$ eV/atom. The maximum force on the atoms is below 0.05 eV/Å and the maximum displacement tolerance is within 0.002 Å while the maximum stress less than 0.01 GPa.

# 3　Results and discussion

## 3.1　Structural properties

MgLa is CsCl type cubic structure with space group PM-3M (No. 221), Mg and La atoms locate on the 1b and 1a Wyckoff sites, respectively. $Mg_2La$ is $MgCu_2$ type cubic structure with space group FD-3M (No. 227), Mg and La atoms locate on the 16d and 8a Wyckoff sites, respectively. $Mg_3La$ is $BiF_3$ type cubic structure with space group FM-3M (No. 225), La atoms occupy 4a Wyckoff site, and Mg atoms the 4b and 8c sites, respectively. The crystal structure of $Mg_xLa$ (x=1, 2, 3) compounds are shown in Fig.1.
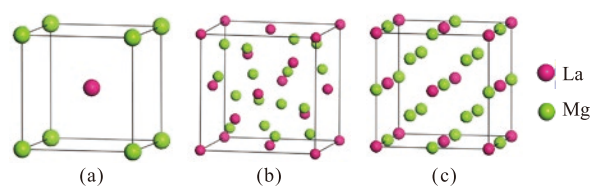


Fig.1　The crystal structures of MgLa (a), $Mg_2La$ (b) and $Mg_3La$ (c)

To ensure accurate calculation results, we used GGA-PBE functional to obtain the equilibrium lattice constants of the ground state of $Mg_xLa$ (x=1, 2, 3) after optimizing crystal structures, and the calculated lattice parameters are shown in Table 1. It can be seen that our results consist well with the experimental results[18-20] by a deviation of less than 1%, and they are also well in agreement with other calculated values[9,11,21]. It is confirmed that the proposed computational methodology is available and the calculated results are dependable.

The equilibrium volume at various pressure ranging from 0 to 30 GPa with a step of 5 GPa of 0 K are optimized and calculated, and variations of the volume with pressures are presented in Fig.2. It can be seen that the ratio of $V/V_0$ decreases for all compounds when external pressure increases, indicating that the greater the external pressure, the smaller the distance between atoms, which leads to the three compounds being difficult to compress with pressure going up mainly because the repulsive interaction between atoms would strengthen as distance reducing. In addition, the lattice parameters of MgLa are the most sensitive to applied external pressure change.

Table 1　Lattice constants of $Mg_xLa$ (x=1, 2, 3) compounds under zero pressure/Å

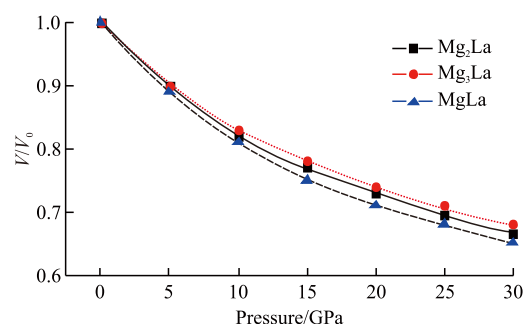| Phase | Species | Present | Cal. | Exp. |
|---|---|---|---|---|
| MgLa | *a* | 4.003 | 3.966[11] | 3.970[18] |
| $Mg_2La$ | *a* | 8.851 | 8.771[21] | 8.806[19] |
| $Mg_3La$ | *a* | 7.539 | 7.507[9] | 7.494[20] |



Fig.2　The volume ratio $V/V_0$ as function of pressure for $Mg_xLa$ (x=1, 2, 3) compounds

## 3.2 Electronic properties

We calculated the electronic structures to have a further insight into the bonding and reveal the underlying fundamental structural stability mechanism of $Mg_xLa$ (x=1, 2, 3). The total and partial densities of states (TDOS and PDOS) at zero pressure are shown in Fig. 3. We can see that the density of states at the Fermi energy is nonzero for all compounds, suggesting that they all exhibit metallic characteristics. It is found that the main bonding peaks of these compounds basically locate in energy range from -7 to 15 eV, and originate from the contribution of valence electron numbers of Mg(s), Mg(p), La(s), La(p) and La(d) orbits for all compounds. All the PDOS also show that the main characteristic of electronic structure of $Mg_xLa$ (x=1, 2, 3) are dominated by the hybridization between Mg(p) orbital and La(d) orbital. Therefore, $Mg_xLa$ (x = 1, 2, 3) exhibit a strong covalent bond.
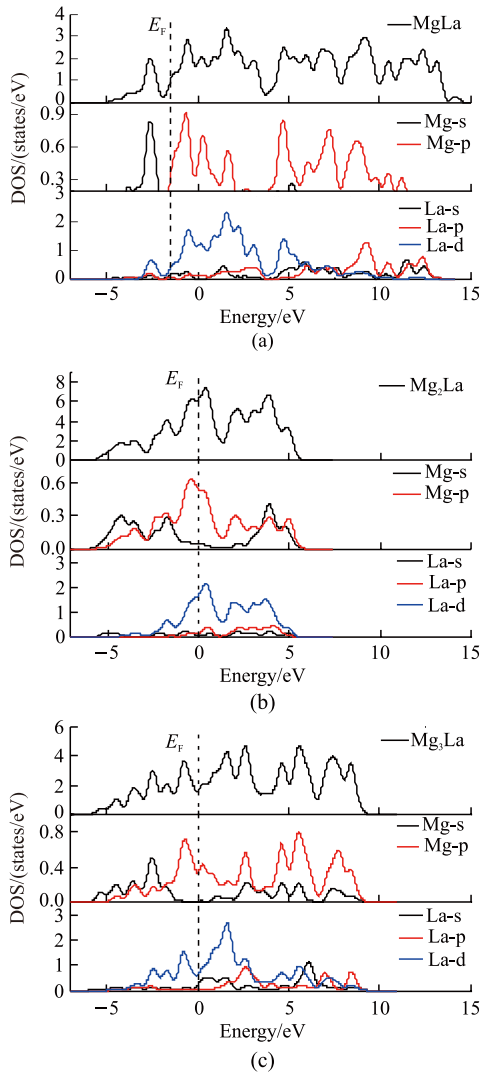
Fig.3 Density of state of MgLa (a), Mg₂La (b) and Mg₃La (c) at 0 GPa

In order to explore the electronic structure change with pressure, the TDOS of Mg$_x$La ($x$=1, 2, 3) under pressure are calculated and plotted in Fig.4. It can be seen that the shape of TDOS curves of the compounds presents tiny changes, indicating that the structures of these compounds have no dramatic changes and there is no structural phase transformation under the pressure up to 30 GPa. Moreover, the peaks of these compounds decrease and broaden with the increase of pressure, indicating that the non-localization of electrons under pressure is strengthened because the fact that the distance between atoms reduces under the pressure, but the overlap of electron clouds between atoms and the freedom of free electrons increase.

In addition, the value of the density of states at the Fermi level can be used to characterize the changes of the stability of the three compounds with increasing pressure. When the Fermi level is at the lowest position of the density of states, the system reaches the most stable state[22]. Our calculated values of the density of

states at Fermi level, N($E_f$) under the pressure of 0, 10, 20 and 30 GPa for MgLa compound are 1.773, 1.092, 0.853 and 0.816 electron/eV, for Mg₂La, the values are 6.229, 4.714, 4.014 and 3.394 electron/eV, while the values are 1.540, 1.265, 1.257 and 1.186 electron/eV for Mg₃La, respectively. Thus, the structural stability of the three compounds increases with the pressure increasing.
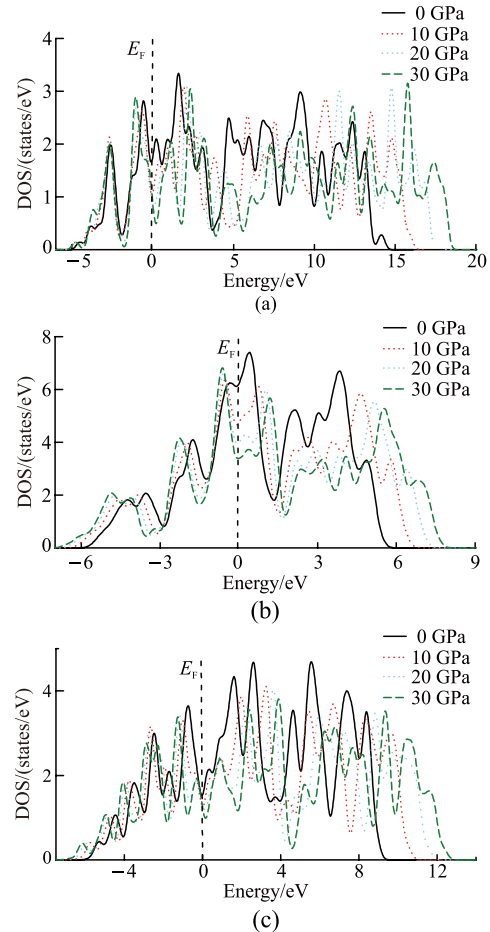


Fig.4  The total density of states of MgLa (a), Mg₂La (b) and Mg₃La (c) under various pressure

## 3.3 Mechanical properties

The elastic constants can be used to reflect the resistance of a crystal under external stress, and thus play an important role in determining mechanical properties concerning the response to pressure. For cubic crystals, there are three independent elastic constants: $C_{11}$, $C_{12}$ and $C_{44}$. The elastic constants $C_{ij}$ of Mg$_x$La ($x$=1, 2, 3) compounds at 0-30 GPa are calculated. Table 2 gives the calculated elastic constants at zero pressure and Fig.5 also plotted the elastic constants at 0-30 GPa. It can be seen in Table 2 that our calculated results are in good agreement with other available theoretical calculations data[9,11,23], which

suggests the computational methodology is feasible and accurate again.

**Table 2  Calculated elastic constants $C_{ij}$ for Mg$_x$La($x$=1, 2, 3) under zero pressure/GPa**

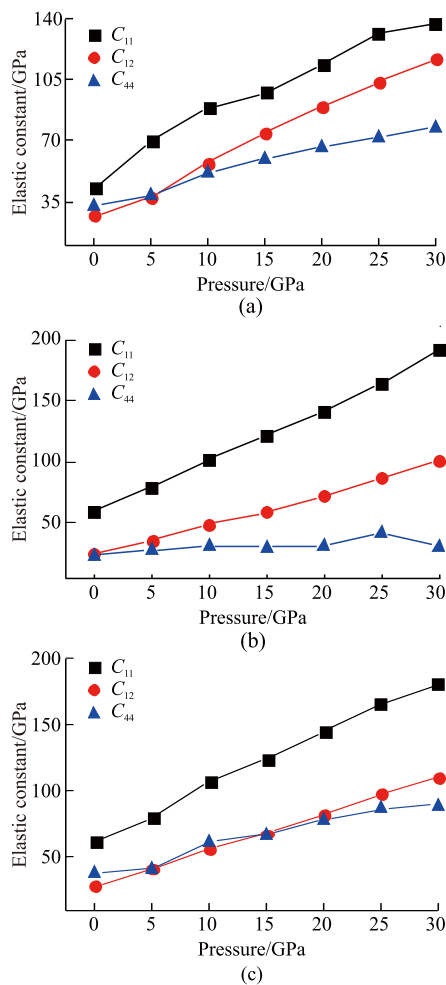| Phase | | $C_{11}$ /GPa | $C_{12}$ /GPa | $C_{44}$ /GPa | $B$ /GPa | $G$ /GPa | $E$ /GPa | $G/B$ |
|---|---|---|---|---|---|---|---|---|
| MgLa | Present | 42.4 | 27.4 | 33.1 | 32.5 | 18.4 | 46.5 | 0.569 |
|  | Cal.[11] | 46.7 | 27.8 | 36.2 | 34.1 | 25.5 | 61.2 | - |
| Mg$_2$La | Present | 59.5 | 25.6 | 23.9 | 36.9 | 20.8 | 52.6 | 0.564 |
|  | Cal.[11] | 58.4 | 24.9 | 21.8 | 36.0 | 19.7 | 50.1 | - |
| Mg$_3$La | Present | 62.3 | 28.2 | 38.3 | 39.6 | 27.7 | 67.3 | 0.699 |
|  | Cal.[9] | 57.9 | 27.1 | 36.2 | 37.4 | 25.7 | 62.7 | - |
|  | Cal.[23] | 59.3 | 26.5 | 36.6 | 37.4 | 26.5 | 64.3 | - |



Fig.5  The elastic constants of MgLa (a), Mg$_2$La (b) and Mg$_3$La (c) compounds under different pressure

As is known to all, the mechanical stability criteria for cubic crystals are listed below[24]:

$$C_{11}-C_{12}>0, \ C_{11}>0, \ C_{44}>0, \ C_{11}+2C_{12}>0 \qquad (1)$$

In Table 2 and Fig.5, the calculated elastic constants of Mg$_x$La($x$=1, 2, 3) compounds obey the cubic mechanical stability criteria when pressure

ranges from 0 to 30 GPa, indicating all the compounds are mechanically stable and no phase transformation occurs at pressure up to 30 GPa. Obviously, the elastic constants $C_{ij}$ almost increase linearly with increasing external pressure, and $C_{11}$ is the most sensitive to applied pressure among the three elastic constants but $C_{44}$ is the most insensitive for the same compounds, which can be verified from the variation ratios of $C_{11}$, $C_{12}$ and $C_{44}$ to pressure ($i\ e$, $\Delta C_{ij}\ /\Delta P$) in 0-30 GPa : 314.7%, 297.0% and 147.0% for MgLa, 441.5%, 253.9% and 22.9% for Mg$_2$La, 377.4%, 272.8% and 169.3% for Mg$_3$La.

Besides, the bulk modulus $B$, shear modulus $G$ and Young's modulus $E$ can be calculated from the three elastic constants $C_{11}$, $C_{12}$ and $C_{44}$ by the Voigt-Reuss-Hill approximation (VRH). These quantities are calculated using the following equations[25,26]:

$$B = \frac{C_{11}+2C_{12}}{3} \qquad (2)$$

$$G_V = \frac{(C_{11}-C_{12}+3C_{44})}{5} \qquad (3)$$

$$\frac{5}{G_R} = \frac{4}{C_{11}-C_{12}} + \frac{3}{C_{44}} \qquad (4)$$

$$G = \frac{G_V+G_R}{2} \qquad (5)$$

$$E = \frac{9GB}{G+3B} \qquad (6)$$

$$\nu = \frac{3B-2G}{2(3B+G)} \qquad (7)$$

Table 2 gives the mechanical parameters of the three compounds at 0 GPa. Unfortunately, no more available experimental data can offer us, so we compare with some other theoretical works[9,11,23]. There is a light difference between them, probably due to different methods of calculations. The calculated bulk modulus $B$, shear modulus $G$, Young's modulus $E$ and $G/B$ values at various pressure are plotted in Fig.6. Generally speaking, a simple relationship empirically links the mechanical properties of materials with their elastic modulus[27], and the bulk modulus $B$ can represent the volume change resistance under pressure[28]. It can be seen from Fig.6 that the values of $B$ of the three compounds almost linearly increase with increasing pressure up to 30 GPa, indicating the resistance to

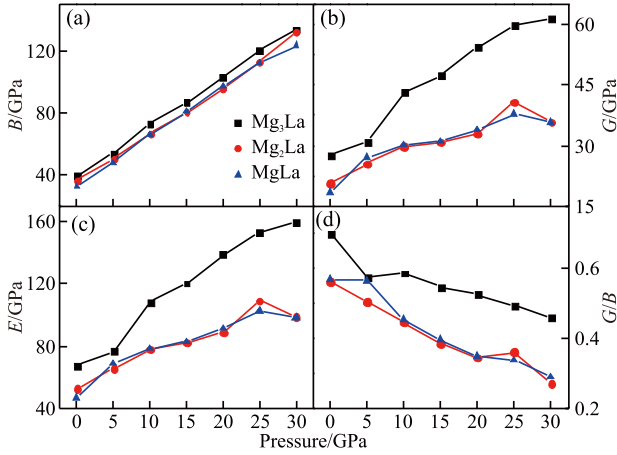volume deformation can be improved by rising external pressure.



Fig.6  The pressure dependence of bulk modulus $B$(a), shear modulus $G$(b), Young's modulus $E$(c) and $G/B$(d) of $Mg_xLa$($x$=1, 2, 3) compounds

The shear modulus $G$ and Young's modulus $E$ play more important role in determining the shear deformation resistance and elastic stiffness of materials, respectively. Generally, the larger $G$ and $E$ are, the harder the materials are[29]. As shown in Fig.6, the shear deformation resistance and elastic stiffness of MgLa and $Mg_2La$ increase at first and then decrease when pressure is up 25 GPa. But the $G$ and $E$ of $Mg_3La$ increase with the increasing pressure, which means the shear deformation resistance and elastic stiffness can be enhanced by rising external pressure. In addition, $Mg_3La$ has the highest $G$ and $E$, indicating that its shear deformation resistance and elastic stiffness are stronger than others.

According to empirical formula of Pugh[27], the ratio of the shear modulus to bulk modulus $G/B$ can predict the brittle and ductile behavior of materials. The critical value which separates the brittle and ductile is about 0.57. If the $G/B$ < 0.57, the materials will have ductitle behavior, otherwise, the materials show brittle behavior. The $G/B$ values of the three compounds change with pressure as shown in Fig.6(d). MgLa and $Mg_2La$ show ductile behavior in 0-30 GPa due to the $G/B$ < 0.57. The $G/B$ values of MgLa continue to decrease in 0-30 GPa with the increasing pressure, which indicates that its ductility can be enhanced by rising external pressure. The $G/B$ of $Mg_2La$ almost linearly reduces with pressure up to 20 GPa, which illustrates that pressure can improve the ductility. $Mg_3La$ displays brittle nature at 0 GPa, but it shows a ductile behavior and continuously enhances with increasing pressure in 5-30 GPa, which indicates that brittle behavior turning

into ductile behavior occurs in 0-5 GPa. In addition, it can be seen easily from the comparison in the figure that the ductile nature of $Mg_3La$ is the worst among the three compounds in 0-30 GPa.

The elastic anisotropy is also an important parameter that can influence on the nanoscale precursor textures in alloys. It is correlated with the possibility of inducing micro-cracks in materials[30]. Here, we use Ranganathan's formula to predict the universal anisotropy index $A^{U}$[31]:

$$A^{U} = 5\frac{G_{V}}{G_{R}} + \frac{B_{V}}{B_{R}} - 6 \qquad (8)$$

where $A^{U}$ is equal to zero means the material shows isotropic, otherwise, the material shows anisotropy. Table 3 lists the calculated universal anisotropy index $A^{U}$ of $Mg_xLa$($x$=1, 2, 3) compounds under some pressures. It is obvious that the three compounds are anisotropic because their values of $A^{U}$ are not equal to zero. And the elastic anisotropy gradually decreases as the order of MgLa>$Mg_3La$>$Mg_2La$ at the same pressure, which indicates that the MgLa is most likely to induce micro-cracks among these compounds with external pressure because of its maximum elastic anisotropy. It can be seen that the values of $A^{U}$ decrease at first and then increase with increasing pressure except $Mg_3La$, which illustrates that the anisotropy of these compounds would show different pressure dependences. Furthermore, MgLa gets the biggest impact on anisotropy under the changing external pressure.

Table 3  The calcucated anisotropic parameters of $Mg_xLa$($x$=1, 2, 3) compounds at different pressure

| Phase | Species | Pressure/GPa | | | |
|---|---|---|---|---|---|
| | | 0 | 10 | 20 | 30 |
| MgLa | $A^{U}$ | 3.156 | 2.557 | 4.514 | 6.873 |
| $Mg_2La$ | $A^{U}$ | 0.142 | 0.042 | 0.006 | 0.178 |
| $Mg_3La$ | $A^{U}$ | 0.834 | 0.982 | 1.076 | 1.110 |

In order to further study the detailed characteristics of elastic anisotropy, 3D Young's modulus $E$ surfaces of three cubic compounds were investigated, which can be obtained from the following equation[32]:

$$\frac{1}{E} = S_{11} - 2(S_{11} - S_{12} - \frac{S_{44}}{2})(l_1^2 l_2^2 + l_2^2 l_3^2 + l_1^2 l_3^2) \qquad (9)$$

where $S_{ij}$ stands for the compliance coefficients, and $l_1$, $l_2$ and $l_3$ denote the direction cosines with respect to the $x$, $y$ and $z$ directions, respectively. Fig.7 shows the 3D Young's modulus $E$ surface of $Mg_xLa$($x$ = 1, 2, 3) at 0, 20, 30 GPa. If the surface is a spherical shape,
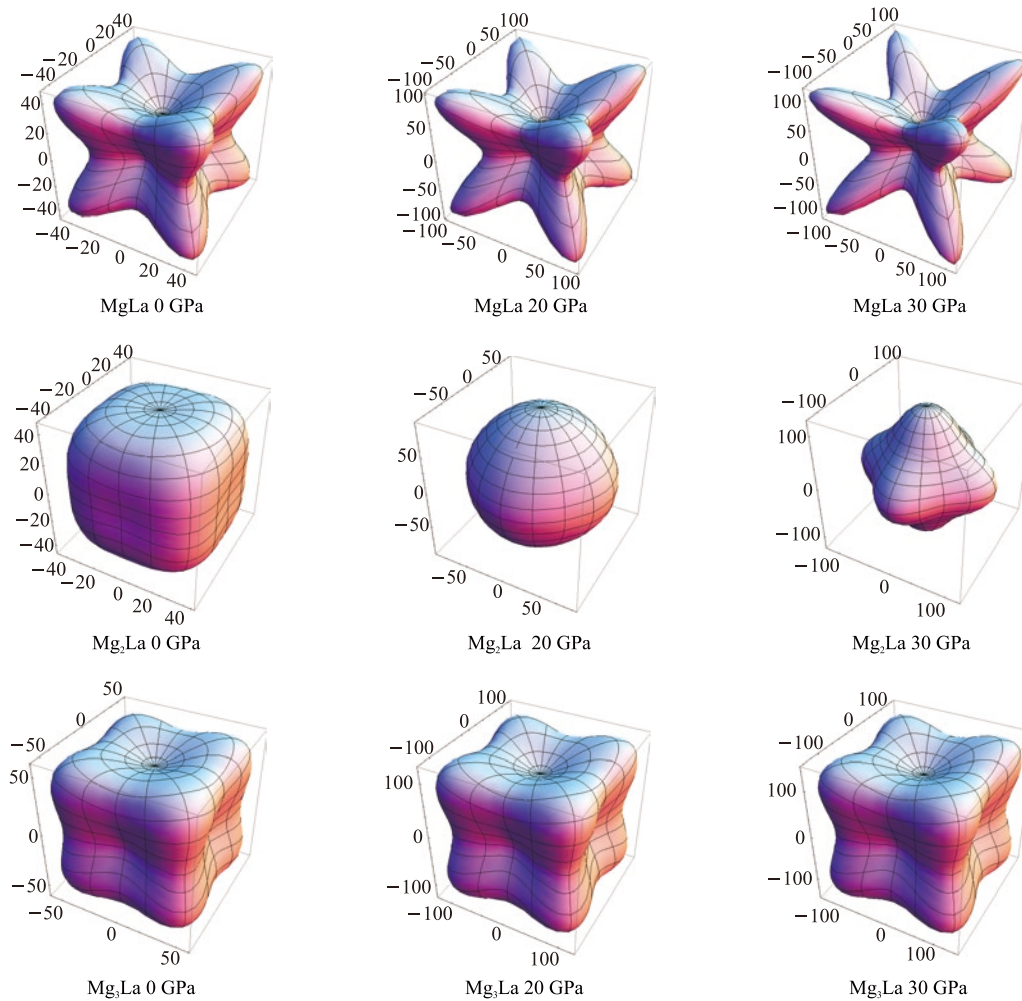
Fig.7 The 3D Young's modulus $E$ surface of $Mg_xLa(x=1, 2, 3)$ at different pressure

the material is isotropic. It can be seen from the 3D curved surfaces that all the compounds perform elastic anisotropy because their 3D surfaces are all deviated from the spherical shape. In addition, the elastic anisotropy of MgLa and $Mg_3La$ increase with external pressure because of the bigger and bigger deviation degree, while $Mg_3La$ exhibits smaller change. These all suggest that the pressure has a great influence on the anisotropy of $Mg_xLa(x = 1, 2, 3)$, and the micro-cracks are easily induced under the increasing pressure. But the impact with pressure on $Mg_3La$ is not obvious.

## 4 Conclusions

The first-principles calculations have been used to study the structural, electronic and mechanical properties of $Mg_xLa(x=1, 2, 3)$ compounds under pressure from 0 to 30 GPa. The main conclusions are as follows:

a) The obtained equilibrium lattice parameters are in well agreement with the available experimental data and theoretical values at 0 GPa. The structural parameters $V/V_0$ decrease with the increase of pressure.

b) The calculated result of DOS shows that the $Mg_xLa$ ($x=1, 2, 3$) compounds have no structural phase transformation in 0-30 GPa. The structural stability of the three phases can be enhanced with increasing pressure.

c) All compounds are mechanically stable in 0-30 GPa, and pressure can enhance their volume resistance. Appropriate pressure can also improve the shear deformation resistance and elastic stiffness of $Mg_3La$. However, the hardness of MgLa and $Mg_2La$ decreases with the pressure range from 25 to 30 GPa.

d) The ductility of MgLa can be improved by rising appropriate external pressure, while brittle behavior turns into ductile behavior in 0-5 GPa for $Mg_3La$. All three compounds exhibit the elastic anisotropy with pressure, while $Mg_3La$ shows few changes with pressure increasing. The pressure has the most sensitive effect on mechanical properties of MgLa.

## References

[1] Mordike B L, Ebert T. Magnesium: Properties-applications Potential[J]. *Mater. Sci. Eng., A*, 2001, 302 (1): 37-45

[2] Potzies C, Kainer K U. Fatigue of Magnesium Alloys[J]. *Adv. Eng. Mater.*, 2004, 6(5): 281-289

[3] Kulekci M K. Magnesium and Its Alloys Applications in Automotive Industry[J]. *Int. J. Adv. Manuf. Technol.*, 2009, 39(9-10): 851-865

[4] Mordike B L. Creep-Resistant Magnesium Alloys[J]. *Mater. Sci. Eng. A*, 2002, 324(1): 103-112

[5] Agnew S R, Nie J F. Preface to the Viewpoint Set on: The Current State of Magnesium Alloy Science and Technology[J]. *Scr. Mater.*, 2010, 63(7): 671-673

[6] Fan J P, Fang L L, Xu B S. Effect of Trace Element La on Microstructure and Properties of Mg-8Al-4Sr-1Y Alloy[J]. *Trans. Mater. Heat Treat.*, 2015, 36(3): 125-129

[7] Liu W J, Cao F H, Chang L R, *et al*. Effect of Rare Earth Element Ce and La on Corrosion Behavior of AM60 Magnesium Alloy[J]. *Corros. Sci.*, 2009, 51 (6): 1 334-1 343

[8] Wei S H, Chen Y G, Tang Y B, *et al*. Compressive Creep Behavior of Mg-Sn-La Alloys[J]. *Mater. Sci. Eng. A*, 2009, 508(1): 59-63

[9] Zhang X D, Wei J J. Elastic, Lattice Dynamical, Thermal Stabilities and Thermodynamic Properties of BiF$_3$-type Mg$_3$RE Compounds from First-Principles Calculations[J]. *Alloys Compd.*, 2016, 663: 565-573

[10] Chen Q, Huang Z W, Zhao Z D, *et al*. Thermal Stabilities, Elastic Properties and Electronic Structures of B2-MgRE (RE = Sc, Y, La) by First-Principles Calculations[J]. *Comput. Mater. Sci.*, 2013, 67: 196-202

[11] Ganeshan S, Shang S L, Zhang H, *et al*. Elastic Constants of Binary Mg Compounds from First-Principles Calculations[J]. *Intermetallics*, 2009, 17(5): 313-318

[12] Perdew J P. Density-Functional Approximation for the Correlation Energy of the Inhomogeneous Electron Gas[J]. *Phys. Rev. B*, 1986, 33(12): 8 822-8 824

[13] Shi D M, Wen B, Melnik R. First-Principles Studies of Al-Ni Intermetallic Compounds[J]. *J. Solid State Chem.*, 2009, 182(10): 2 664-2 669

[14] Laasonen K, Pasquarello A, Car R, *et al*. Car-Parrinellomolecular Dynamics with Vanderbilt Ultrasoft Pseudopotentials[J]. *Phys. Rev. B*, 1993, 47: 10 142

[15] Pack J D, Monkhors H J. Special Points for Brillouin-zone Integrations[J]. *Phys. Rev. B*, 1977, 16: 1 748-1 749

[16] Perdew J P, Burke K, Ernzerh M. Generalized Gradient Approximation Made Simple[J]. *Phys. Rev. Lett.*, 1996, 77(18): 3 865-3 868

[17] Fischer T H, Almlof J. General Methods for Geometry and Wave Function Optimization[J]. *J. Phys. Chem.*, 1992, 96(24): 9 768-9 774

[18] Iandelli A, Palenzona A. Atomic Size of Rare Earths in Intermetallic Compounds. MX Compounds of CsCl Type[J]. *J. Less-Common Met.*, 1965, 9(1): 1-6

[19] Giovannin M, Marazza R, Saccone A, *et al*. Isothermal Section from 50 at% to 75 at% Mg of the Ternary System Y-La-Mg[J]. *J. Alloys Compd.*, 1994, 203: 177-180

[20] Yang F, Wang J W, Ke J L, *et al*. Elastic Properties and Electronic Structures of Mg-Ce Intermetallic Compounds from First-Principles Calculations[J]. *Phys. Status Solid B*, 2011, 248(9): 2 097-2 102

[21] Ouyang Y, Tao X M, Chen H M, *et al*. First-Principles Calculations of Mechanical and Thermodynamic Properties of the Laves-MgRE (RE = La, Ce, Pr, Nd, Pm, Sm, Gd)[J]. *Comput. Mater. Sci.*, 2010, 47(2): 297-301

[22] Hong T, Watsonyang T J, Freeman A J, *et al*. Crystal Structure, Phase Stability, and Electronic Structure of Ti-Al Intermetallics: TiAl$_3$[J]. *Phys. Rev. B*, 1990, 41(18): 12 462

[23] Wrobel J, Hector L G, Wolf W, *et al*. Thermodynamic and Mechanical Properties of Lanthanum-Magnesium Phases from Density Functional Theory[J]. *J. Alloys Compd.*, 2012, 512(1): 296-310

[24] Grimvall G. *Thermophysical Properties of Materials*[M]. North Holland: Elsevier, 1999

[25] Hill R. The Elastic Behaviour of a Crystalline Aggregate[J]. *Proc. Phys. Soc. A*, 1952, 65(5): 349-354

[26] Reuss A. Berechnung der Fließgrenze von Mischkristallen auf Grund der Plastizitätsbedingung für Einkristalle[J]. *Z. Angew. Math. Mech*, 1929, 9 (1): 49-58

[27] Pugh S F. Relations between the Elastic Moduli and the Plastic Properties of Polycrystalline Pure Metals[J]. *Philos. Mag.*, 1954, 45: 823-843

[28] Vaitheeswaran G, Kanchana V, Kumar R S, *et al*. High-Pressure Structural, Elastic, and Electronic Properties of the Scintillator Host Material KMgF$_3$[J]. *Phys. Rev. B*, 2007, 76(1): 014 107

[29] Gao L, Zhou J, Sun Z M, *et al*. Electronic Origin of the Anomalous Solid Solution Hardening of Y and Gd in Mg:A First-Principles Study[J]. *Chin. Sci. Bull.*, 2011, 56(10): 1 038-1 042

[30] Tvergaard V, Hutchinson J W. Microcracking in Ceramics Induced by Thermal Expansion or Elastic Anisotropy[J]. *J. Am. Ceram. Soc.*, 2010, 71(3): 157-166

[31] Ranganathan S I, Ostoja-Starzewski M. Universal Elastic Anisotropy Index[J]. *Phys. Rev. Lett.*, 2008, 101: 055 504

[32] Nye J F. *Physical Properties of Crystals*[M]. Oxford: Oxford University Press, 1985